Extension of SBL Algorithms for the Recovery of Block Sparse Signals with Intra-Block Correlation

Zhilin Zhang, *Student Member, IEEE* and Bhaskar D. Rao, *Fellow, IEEE*

Abstract

We examine the recovery of block sparse signals and extend the framework in two important directions; one by exploiting signals' intra-block correlation and the other by generalizing signals' block structure. We propose two families of algorithms based on the framework of block sparse Bayesian learning (BSBL). One family, directly derived from the BSBL framework, requires knowledge of the block structure. Another family, derived from an expanded BSBL framework, is based on a weaker assumption on the block structure, and can be used when the block structure is completely unknown. Using these algorithms we show that exploiting intra-block correlation is very helpful in improving recovery performance. These algorithms also shed light on how to modify existing algorithms or design new ones to exploit such correlation and improve performance.

Index Terms

Sparse Signal Recovery, Compressed Sensing, Block Sparse Model, Sparse Bayesian Learning (SBL), Intra-Block Correlation

I. Introduction

Sparse signal recovery and the associated problems of compressed sensing have received much attention in recent years [1]. The basic model is given by

$$\mathbf{y} = \mathbf{\Phi}\mathbf{x} + \mathbf{v}, \tag{1}$$

Z.Zhang and B.D.Rao are with the Department of Electrical and Computer Engineering, University of California, San Diego, La Jolla, CA 92093-0407, USA. Email: zhangzlacademy@gmail.com (Z.Z), brao@ucsd.edu (B.D.R). The work was supported by NSF grants CCF-0830612 and CCF-1144258.

where $\mathbf{y} \in \mathbb{R}^{M \times 1}$ is a known measurement vector, $\mathbf{\Phi} \in \mathbb{R}^{M \times N} (M \ll N)$ is a known matrix (generally called the sensing matrix) and any M columns are linearly independent, $\mathbf{x} \in \mathbb{R}^{N \times 1}$ is a sparse signal which we want to recover, and $\mathbf{v}$ is a noise vector. In applications, $\mathbf{x}$ generally has additional structure. A widely studied structure is block/group structure [2]–[4]. With this structure, $\mathbf{x}$ can be viewed as a concatenation of g blocks, i.e.,

$$\mathbf{x} = [\underbrace{x_1, \cdots, x_{d_1}}_{\mathbf{x}_1^T}, \cdots, \underbrace{x_{d_{g-1}+1}, \cdots, x_{d_g}}_{\mathbf{x}_g^T}]^T \tag{2}$$

where $d_i (\forall i)$ are not necessarily identical. Among the g blocks, only k ($k \ll g$) blocks are nonzero but their locations are unknown. It is known that exploiting such block partition can further improve recovery performance.

A number of algorithms have been proposed to recover sparse signals with the block structure. Typical algorithms include Model-CoSaMp [3], Block-OMP [4], and Group-Lasso type algorithms such as the original Group Lasso algorithm [2], Group Basis Pursuit [5], and the Mixed ℓ_2/ℓ_1 Program [6]. These algorithms require knowledge of the block partition (2). Other algorithms such as StructOMP [7], do not need to know the block partition but need to know other *a priori* information, e.g., the number of nonzero elements in $\mathbf{x}$. Recently, CluSS-MCMC [8] and BM-MAP-OMP [9] have been proposed, which require very little a priori knowledge.

However, few existing algorithms consider intra-block correlation, i.e., the correlation among amplitudes of the elements within each block. In practical applications the intra-block correlation widely exists, such as physiological signals [10] and images. In this work we derive several algorithms that explore and exploit the intra-block correlation to improve performance. These algorithms are based on our recently proposed block sparse Bayesian learning (BSBL) framework [11]. Although the framework was initially used to derive algorithms for multiple measurement vector (MMV) models [12], it has not been used for the block sparse model (1)-(2). The successes of sparse Bayesian learning methods in past contexts motivate us to consider their extension to this problem and fill this gap.

One contribution of our work is that the proposed algorithms are the first ones in the category that adaptively explore and exploit the intra-block correlation. Experiments showed that the developed algorithms significantly outperform competitive algorithms. We also suggest a promising strategy to incorporate the intra-block correlation in the Group-Lasso type algorithms to improve their performance.

Another contribution is the insight into the effect of the intra-block correlation on algorithms' performance. An MMV model can be viewed as a special case of a block sparse model. But we found the effect of the intra-block correlation on algorithmic performance is quite different from the effect of the temporal correlation [11].

The third contribution is the development of a simple approximate model and corresponding algorithms to solve the problem when the block partition is entirely unknown. These algorithms are effective especially in noisy environments.

In this paper bold symbols are reserved for vectors and matrices. For square matrices $\mathbf{A}_1, \cdots, \mathbf{A}_g$, $\mathrm{diag}\{\mathbf{A}_1, \cdots, \mathbf{A}_g\}$ denotes a block diagonal matrix with principal diagonal blocks being $\mathbf{A}_1, \cdots, \mathbf{A}_g$ in turn. $\mathrm{Tr}(\mathbf{A})$ denotes the trace of $\mathbf{A}$. $\boldsymbol{\gamma} \succeq \mathbf{0}$ means each element in the vector $\boldsymbol{\gamma}$ is nonnegative.

Parts of this work have been published in [13].

II. Overview of the BSBL Framework

This section briefly describes the BSBL framework [11], upon which we develop our algorithms. In this framework, each block $\mathbf{x}_i \in \mathbb{R}^{d_i \times 1}$ is assumed to satisfy a parameterized multivariate Gaussian distribution:

$$p(\mathbf{x}_i; \gamma_i, \mathbf{B}_i) \sim \mathcal{N}(\mathbf{0}, \gamma_i \mathbf{B}_i), \quad i = 1, \cdots, g$$

with the unknown parameters γ_i and $\mathbf{B}_i$. Here γ_i is a nonnegative parameter controlling the block-sparsity of $\mathbf{x}$. When $\gamma_i = 0$, the i-th block becomes zero. During the learning procedure most γ_i tend to be zero, due to the mechanism of automatic relevance determination [14]. Thus sparsity at the block level is encouraged. $\mathbf{B}_i \in \mathbb{R}^{d_i \times d_i}$ is a positive definite matrix, capturing the correlation structure of the i-th block. Under the assumption that blocks are mutually uncorrelated, the prior of $\mathbf{x}$ is $p(\mathbf{x}; \{\gamma_i, \mathbf{B}_i\}_i) \sim \mathcal{N}(\mathbf{0}, \mathbf{\Sigma}_0)$, where $\mathbf{\Sigma}_0 = \mathrm{diag}\{\gamma_1 \mathbf{B}_1, \cdots, \gamma_g \mathbf{B}_g\}$. Assume the noise vector satisfies $p(\mathbf{v}; \lambda) \sim \mathcal{N}(\mathbf{0}, \lambda \mathbf{I})$, where λ is a positive scalar. Therefore the posterior of $\mathbf{x}$ is given by $p(\mathbf{x}|\mathbf{y}; \lambda, \{\gamma_i, \mathbf{B}_i\}_{i=1}^g) = \mathcal{N}(\boldsymbol{\mu}_x, \mathbf{\Sigma}_x)$ with $\boldsymbol{\mu}_x = \mathbf{\Sigma}_0 \mathbf{\Phi}^T \big(\lambda \mathbf{I} + \mathbf{\Phi} \mathbf{\Sigma}_0 \mathbf{\Phi}^T\big)^{-1} \mathbf{y}$ and $\mathbf{\Sigma}_x = (\mathbf{\Sigma}_0^{-1} + \frac{1}{\lambda} \mathbf{\Phi}^T \mathbf{\Phi})^{-1}$. Once the parameters $\lambda, \{\gamma_i, \mathbf{B}_i\}_{i=1}^g$ are estimated, the Maximum-A-Posteriori (MAP) estimate of $\mathbf{x}$, denoted by $\widehat{\mathbf{x}}$, can be directly obtained from the mean of the posterior, i.e.,

$$\widehat{\mathbf{x}} \leftarrow \mathbf{\Sigma}_0 \mathbf{\Phi}^T \big(\lambda \mathbf{I} + \mathbf{\Phi} \mathbf{\Sigma}_0 \mathbf{\Phi}^T\big)^{-1} \mathbf{y}.$$

The parameters can be estimated by a Type II maximum likelihood procedure [14]. This is equivalent to minimizing the following cost function [11]

$$\mathcal{L}(\Theta) \triangleq \log |\lambda \mathbf{I} + \mathbf{\Phi} \mathbf{\Sigma}_0 \mathbf{\Phi}^T| + \mathbf{y}^T (\lambda \mathbf{I} + \mathbf{\Phi} \mathbf{\Sigma}_0 \mathbf{\Phi}^T)^{-1} \mathbf{y}, \tag{3}$$

where Θ denotes all the parameters $\lambda, \{\gamma_i, \mathbf{B}_i\}_{i=1}^g$. This framework is called the BSBL framework [11].

Each algorithm derived from this framework includes three learning rules, i.e., the learning rules for γ_i, $\mathbf{B}_i$, and λ. The learning rule for γ_i is the main body of an algorithm. Different γ_i learning rules lead to different convergence speed [1], and determine the best possible recovery performance when optimal values of λ and $\mathbf{B}_i$ are given.

The λ learning rule is important as well. If an optimal (or a good sub-optimal) value for λ cannot be obtained, the recovery performance can be very poor even if the γ_i learning rule could potentially lead to perfect recovery performance.

As for $\mathbf{B}_i(\forall i)$, it can be shown [11] that in noiseless environments, the global minimum of (3) always leads to the true sparse solution irrespective of the value of $\mathbf{B}_i$; $\mathbf{B}_i$ only affects local convergence (such as changing the shape of the basins of attraction of local minima). Therefore, one can impose various constraints on the form of $\mathbf{B}_i$ to achieve better performance and prevent overfitting.

An interesting property of the framework is that it is capable of directly recovering less-sparse or non-sparse signals as shown in [10].

III. Algorithms When the Block Partition is Known

In this section we propose three algorithms, which require knowledge of the block partition (2).

A. BSBL-EM: the EM Method

This algorithm can be readily derived from our previous work [11] on MMV models with suitable adaptation. Thus we omit details on algorithm derivation. However, several necessary changes, particularly for enhancing the robustness of the learning rules for λ and $\mathbf{B}_i$, have to be made here.

Following the Expectation Maximization (EM) method [11], we can derive the learning rules for γ_i and λ:

$$\gamma_i \leftarrow \frac{1}{d_i}\mathrm{Tr}\big[\mathbf{B}_i^{-1}\big(\mathbf{\Sigma}_x^i + \boldsymbol{\mu}_x^i(\boldsymbol{\mu}_x^i)^T\big)\big], \quad \forall i \tag{4}$$

$$\lambda \leftarrow \frac{\|\mathbf{y}-\mathbf{\Phi}\boldsymbol{\mu}_x\|_2^2 + \mathrm{Tr}(\mathbf{\Sigma}_x\mathbf{\Phi}^T\mathbf{\Phi})}{M}, \tag{5}$$

where $\boldsymbol{\mu}_x^i \in \mathbb{R}^{d_i\times 1}$ is the corresponding i-th block in $\boldsymbol{\mu}_x$, and $\mathbf{\Sigma}_x^i \in \mathbb{R}^{d_i\times d_i}$ is the corresponding i-th principal diagonal block in $\mathbf{\Sigma}_x$. Note that the λ learning rule (5) is not robust in low SNR cases. By numerical study, we empirically find that this is due in part to the disturbance caused by the off-block-diagonal elements in $\mathbf{\Sigma}_x$ and $\mathbf{\Phi}^T\mathbf{\Phi}$. Therefore, we set their off-block-diagonal elements to zero, leading

[1] The λ learning rule also affects the speed, but its effect is not dominant.

to the learning rule

$$\lambda \;\; \leftarrow \;\; \frac{\|\mathbf{y} - \mathbf{\Phi}\boldsymbol{\mu}_x\|_2^2 + \sum_{i=1}^{g} \mathrm{Tr}(\mathbf{\Sigma}_x^i (\mathbf{\Phi}^i)^T \mathbf{\Phi}^i)}{M}, \tag{6}$$

where $\mathbf{\Phi}^i \in \mathbb{R}^{M \times d_i}$ is the submatrix of $\mathbf{\Phi}$, which corresponds to the i-th block of $\mathbf{x}$. This λ learning rule is better than (5) in generally noisy environments (e.g., $\mathrm{SNR} < 20\mathrm{dB}$). In noiseless cases there is no need to use any λ learning rules. Just fixing λ to a small value, e.g., 10^{-10}, can yield satisfactory performance.

Similar to [11], using the EM method we can derive a learning rule for $\mathbf{B}_i$. However, assigning a different $\mathbf{B}_i$ to each blcok can result in overfitting. When blocks have the same size, an effective strategy to avoid the overfitting is parameter averaging [11], i.e., constraining $\mathbf{B}_i = \mathbf{B}(\forall i)$. Using this constraint, the learning rule for $\mathbf{B}$ can be derived as follows

$$\mathbf{B} \leftarrow \frac{1}{g} \sum_{i=1}^{g} \frac{\mathbf{\Sigma}_x^i + \boldsymbol{\mu}_x^i (\boldsymbol{\mu}_x^i)^T}{\gamma_i}. \tag{7}$$

However, the algorithm's performance can be improved by further constraining the matrix $\mathbf{B}$. The idea is to find a positive definite and symmetric matrix $\widehat{\mathbf{B}}$ such that it is determined by one parameter but is close to $\mathbf{B}$ especially along the main diagonal and the main sub-diagonal. Further, we find that for many applications modeling elements of a block as a first-order Auto-Regressive (AR) process is sufficient to model the intra-block correlation. In this case, the corresponding correlation matrix of the block is a Toeplitz matrix with the following form:

$$\mathrm{Toeplitz}([1, r, \cdots, r^{d-1}]) = \begin{bmatrix} 1 & r & \cdots & r^{d-1} \\ \vdots & & & \vdots \\ r^{d-1} & r^{d-2} & \cdots & 1 \end{bmatrix} \tag{8}$$

where r is the AR coefficient and d is the block size. Here we constrain $\widehat{\mathbf{B}}$ to have this form. Instead of estimating r from the BSBL cost function, we empirically calculate its value by $r \triangleq \frac{m_1}{m_0}$, where m_0 (resp. m_1) is the average of the elements along the main diagonal (resp. the main sub-diagonal) of the matrix $\mathbf{B}$ in (7).

When blocks have different sizes, the above idea can still be used. First, using the EM method we can derive the rule for each $\mathbf{B}_i$: $\mathbf{B}_i \leftarrow \frac{1}{\gamma_i}\left[\mathbf{\Sigma}_x^i + \boldsymbol{\mu}_x^i(\boldsymbol{\mu}_x^i)^T\right]$. Then, for each $\mathbf{B}_i$ we calculate the averages of the elements along the main diagonal and the main sub-diagonal, i.e., m_0^i and m_1^i, respectively, and average m_0^i and m_1^i for all blocks as follows: $\overline{m}_0 \triangleq \sum_{i=1}^{g} m_0^i$ and $\overline{m}_1 \triangleq \sum_{i=1}^{g} m_1^i$. Finally, we have $\overline{r} \triangleq \frac{\overline{m}_1}{\overline{m}_0}$, from which we construct $\widehat{\mathbf{B}}_i$ for the i-th block:

$$\widehat{\mathbf{B}}_i = \mathrm{Toeplitz}([1, \overline{r}, \cdots, \overline{r}^{d_i - 1}]) \quad (\forall i) \tag{9}$$

We denote the above algorithm by **BSBL-EM**.

B. BSBL-BO: the Bound-Optimization Method

The BSBL-EM algorithm has satisfactory recovery performance but is slow. This is mainly due to the EM based γ_i learning rule. For the basic SBL algorithm, Tipping [14] derived a fixed-point based γ_i learning rule to replace the EM based one, which has faster convergence speed but is not robust in some noisy environments. Here we derive a fast γ_i learning rule based on the bound-optimization method (also known as the Majorization-Minimization method) [1], [15]. The algorithm adopting this γ_i learning rule is denoted by **BSBL-BO** (it uses the same learning rules for $\mathbf{B}_i$ and λ as BSBL-EM). It not only has fast speed, but also has satisfactory performance.

Note that the original cost function (3) consists of two terms. The first term $\log|\lambda\mathbf{I}+\mathbf{\Phi}\mathbf{\Sigma}_0\mathbf{\Phi}^T|$ is concave with respect to $\boldsymbol{\gamma}\succeq\mathbf{0}$, where $\boldsymbol{\gamma}\triangleq[\gamma_1,\cdots,\gamma_g]^T$. The second term $\mathbf{y}^T(\lambda\mathbf{I}+\mathbf{\Phi}\mathbf{\Sigma}_0\mathbf{\Phi}^T)^{-1}\mathbf{y}$ is convex with respect to $\boldsymbol{\gamma}\succeq\mathbf{0}$. Since our goal is to minimize the cost function, we choose to find an upper-bound for the first item and then minimize the upper-bound of the cost function.

We use the supporting hyperplane of the first term as its upper-bound. Let $\boldsymbol{\gamma}^*$ be a given point in the $\boldsymbol{\gamma}$-space. We have

$$\begin{aligned}\log|\lambda\mathbf{I}+\mathbf{\Phi}\mathbf{\Sigma}_0\mathbf{\Phi}^T| &\le \log|\lambda\mathbf{I}+\mathbf{\Phi}\mathbf{\Sigma}_0^*\mathbf{\Phi}^T| \\ &\quad +\sum_{i=1}^{g}\mathrm{Tr}\big((\mathbf{\Sigma}_y^*)^{-1}\mathbf{\Phi}^i\mathbf{B}_i(\mathbf{\Phi}^i)^T\big)(\gamma_i-\gamma_i^*) \\ &= \sum_{i=1}^{g}\mathrm{Tr}\big((\mathbf{\Sigma}_y^*)^{-1}\mathbf{\Phi}^i\mathbf{B}_i(\mathbf{\Phi}^i)^T\big)\gamma_i+\log|\mathbf{\Sigma}_y^*| \\ &\quad -\sum_{i=1}^{g}\mathrm{Tr}\big((\mathbf{\Sigma}_y^*)^{-1}\mathbf{\Phi}^i\mathbf{B}_i(\mathbf{\Phi}^i)^T\big)\gamma_i^* \qquad (10)\end{aligned}$$

where $\mathbf{\Sigma}_y^*=\lambda\mathbf{I}+\mathbf{\Phi}\mathbf{\Sigma}_0^*\mathbf{\Phi}^T$ and $\mathbf{\Sigma}_0^*\triangleq\mathbf{\Sigma}_0|_{\boldsymbol{\gamma}=\boldsymbol{\gamma}^*}$. Substituting (10) into the cost function (3) we have

$$\begin{aligned}\mathcal{L}(\boldsymbol{\gamma}) &\le \sum_{i=1}^{g}\mathrm{Tr}\big((\mathbf{\Sigma}_y^*)^{-1}\mathbf{\Phi}^i\mathbf{B}_i(\mathbf{\Phi}^i)^T\big)\gamma_i \\ &\quad +\mathbf{y}^T(\lambda\mathbf{I}+\mathbf{\Phi}\mathbf{\Sigma}_0\mathbf{\Phi}^T)^{-1}\mathbf{y}+\log|\mathbf{\Sigma}_y^*| \\ &\quad -\sum_{i=1}^{g}\mathrm{Tr}\big((\mathbf{\Sigma}_y^*)^{-1}\mathbf{\Phi}^i\mathbf{B}_i(\mathbf{\Phi}^i)^T\big)\gamma_i^* \\ &\triangleq \widetilde{\mathcal{L}}(\boldsymbol{\gamma}) \qquad (11)\end{aligned}$$

The function $\widetilde{\mathcal{L}}(\boldsymbol{\gamma})$ is convex over $\boldsymbol{\gamma}$, and when $\boldsymbol{\gamma}=\boldsymbol{\gamma}^*$ we have $\mathcal{L}(\boldsymbol{\gamma}^*)=\widetilde{\mathcal{L}}(\boldsymbol{\gamma}^*)$. Further, for any $\boldsymbol{\gamma}_{\min}$ which minimizes $\widetilde{\mathcal{L}}(\boldsymbol{\gamma})$, we have the following relationship: $\mathcal{L}(\boldsymbol{\gamma}_{\min})\le\widetilde{\mathcal{L}}(\boldsymbol{\gamma}_{\min})\le\widetilde{\mathcal{L}}(\boldsymbol{\gamma}^*)=\mathcal{L}(\boldsymbol{\gamma}^*)$.

This indicates that when we minimize the surrogate function $\widetilde{\mathcal{L}}(\boldsymbol{\gamma})$ over $\boldsymbol{\gamma}$, the resulting minimum point effectively decreases the original cost function $\mathcal{L}(\boldsymbol{\gamma})$. We can use any optimization software to optimize (11). However, our experiments showed that this takes more time than BSBL-EM and leads to poorer recovery performance. Therefore, we consider another surrogate function. Using the identity

$$\mathbf{y}^T(\lambda \mathbf{I} + \boldsymbol{\Phi}\boldsymbol{\Sigma}_0\boldsymbol{\Phi}^T)^{-1}\mathbf{y} \equiv \min_{\mathbf{x}} \big[\frac{1}{\lambda}\|\mathbf{y} - \boldsymbol{\Phi}\mathbf{x}\|_2^2 + \mathbf{x}^T\boldsymbol{\Sigma}_0^{-1}\mathbf{x}\big], \tag{12}$$

where the optimal $\mathbf{x}$ is $\boldsymbol{\mu}_x$, we have

$$\begin{aligned}\widetilde{\mathcal{L}}(\boldsymbol{\gamma}) \quad = \quad & \min_{\mathbf{x}} \frac{1}{\lambda}\|\mathbf{y} - \boldsymbol{\Phi}\mathbf{x}\|_2^2 + \mathbf{x}^T\boldsymbol{\Sigma}_0^{-1}\mathbf{x} \\ & + \sum_{i=1}^{g} \mathrm{Tr}\big((\boldsymbol{\Sigma}_y^*)^{-1}\boldsymbol{\Phi}^i\mathbf{B}_i(\boldsymbol{\Phi}^i)^T\big)\gamma_i + \log|\boldsymbol{\Sigma}_y^*| \\ & - \sum_{i=1}^{g} \mathrm{Tr}\big((\boldsymbol{\Sigma}_y^*)^{-1}\boldsymbol{\Phi}^i\mathbf{B}_i(\boldsymbol{\Phi}^i)^T\big)\gamma_i^*.\end{aligned}$$

Then, a new function

$$\begin{aligned}\mathcal{G}(\boldsymbol{\gamma}, \mathbf{x}) \quad \triangleq \quad & \frac{1}{\lambda}\|\mathbf{y} - \boldsymbol{\Phi}\mathbf{x}\|_2^2 + \mathbf{x}^T\boldsymbol{\Sigma}_0^{-1}\mathbf{x} \\ & + \sum_{i=1}^{g} \mathrm{Tr}\big((\boldsymbol{\Sigma}_y^*)^{-1}\boldsymbol{\Phi}^i\mathbf{B}_i(\boldsymbol{\Phi}^i)^T\big)\gamma_i \\ & + \log|\boldsymbol{\Sigma}_y^*| - \sum_{i=1}^{g} \mathrm{Tr}\big((\boldsymbol{\Sigma}_y^*)^{-1}\boldsymbol{\Phi}^i\mathbf{B}_i(\boldsymbol{\Phi}^i)^T\big)\gamma_i^*\end{aligned}$$

is defined, which is the upper-bound of $\widetilde{\mathcal{L}}(\gamma)$. Note that $\mathcal{G}(\gamma, \mathbf{x})$ is convex in both γ and $\mathbf{x}$. It can be easily shown that the solution $(\boldsymbol{\gamma}^\diamond)$ of $\widetilde{\mathcal{L}}(\gamma)$ is the solution $(\gamma^\diamond, \mathbf{x}^\diamond)$ of $\mathcal{G}(\gamma, \mathbf{x})$. Thus, $\mathcal{G}(\gamma, \mathbf{x})$ is our final surrogate cost function.

Taking the derivative of $\mathcal{G}$ with respect to γ_i, we can obtain

$$\gamma_i \quad \leftarrow \quad \sqrt{\frac{\mathbf{x}_i^T\mathbf{B}_i^{-1}\mathbf{x}_i}{\mathrm{Tr}\big((\boldsymbol{\Phi}^i)^T(\boldsymbol{\Sigma}_y^*)^{-1}\boldsymbol{\Phi}^i\mathbf{B}_i\big)}}. \tag{13}$$

Due to this γ_i learning rule, BSBL-BO requires far fewer iterations than BSBL-EM, but both algorithms have comparable performance.

C. BSBL-ℓ_1: Hybrid of BSBL and Group-Lasso Type Algorithms

Essentially, BSBL-EM and BSBL-BO operate in the $\boldsymbol{\gamma}$-space, since their cost function is a function of $\boldsymbol{\gamma}$. In contrast, most existing algorithms for the block sparse model (1)-(2) directly operate in the $\mathbf{x}$-space, minimizing a data fit term and a penalty, which are both functions of $\mathbf{x}$. It is interesting to see the relation between our BSBL algorithms and those algorithms.

Using the idea we presented in [16], an extension of the duality space analysis for the basic SBL framework [17], we can transform the BSBL cost function (3) from the $\boldsymbol{\gamma}$-space to the $\mathbf{x}$-space. Since λ and $\mathbf{B}_i(\forall i)$ can be viewed as regularizers, for convenience we first treat them as fixed values.

First, using the identity (12) we can upper-bound the BSBL cost function as follows:

$$\mathfrak{L}(\mathbf{x},\boldsymbol{\gamma}) = \log|\lambda\mathbf{I}+\boldsymbol{\Phi}\boldsymbol{\Sigma}_0\boldsymbol{\Phi}^T| + \frac{1}{\lambda}\|\mathbf{y}-\boldsymbol{\Phi}\mathbf{x}\|_2^2 + \mathbf{x}^T\boldsymbol{\Sigma}_0^{-1}\mathbf{x}.$$

By first minimizing over $\boldsymbol{\gamma}$ and then minimizing over $\mathbf{x}$, we have:

$$\mathbf{x} = \arg\min_{\mathbf{x}} \Big\{\|\mathbf{y}-\boldsymbol{\Phi}\mathbf{x}\|_2^2 + \lambda g_{\mathrm{c}}(\mathbf{x})\Big\}, \tag{14}$$

with the penalty $g_{\mathrm{c}}(\mathbf{x})$ given by

$$g_{\mathrm{c}}(\mathbf{x}) \triangleq \min_{\boldsymbol{\gamma}\succeq\mathbf{0}} \Big\{\mathbf{x}^T\boldsymbol{\Sigma}_0^{-1}\mathbf{x} + \log|\lambda\mathbf{I}+\boldsymbol{\Phi}\boldsymbol{\Sigma}_0\boldsymbol{\Phi}^T|\Big\}. \tag{15}$$

Define $h(\boldsymbol{\gamma}) \triangleq \log|\lambda\mathbf{I}+\boldsymbol{\Phi}\boldsymbol{\Sigma}_0\boldsymbol{\Phi}^T|$. It is concave and non-decreasing w.r.t. $\boldsymbol{\gamma}\succeq\mathbf{0}$. Thus we have

$$\log|\lambda\mathbf{I}+\boldsymbol{\Phi}\boldsymbol{\Sigma}_0\boldsymbol{\Phi}^T| = \min_{\mathbf{z}\succeq\mathbf{0}} \mathbf{z}^T\boldsymbol{\gamma} - h^*(\mathbf{z}) \tag{16}$$

where $h^*(\mathbf{z})$ is the concave conjugate of $h(\boldsymbol{\gamma})$ and can be expressed as $h^*(\mathbf{z}) = \min_{\boldsymbol{\gamma}\succeq\mathbf{0}} \mathbf{z}^T\boldsymbol{\gamma} - \log|\lambda\mathbf{I}+\boldsymbol{\Phi}\boldsymbol{\Sigma}_0\boldsymbol{\Phi}^T|$. Thus, using (16) we can express (15) as

$$\begin{aligned} g_{\mathrm{c}}(\mathbf{x}) &= \min_{\boldsymbol{\gamma},\mathbf{z}\succeq\mathbf{0}} \mathbf{x}^T\boldsymbol{\Sigma}_0^{-1}\mathbf{x} + \mathbf{z}^T\boldsymbol{\gamma} - h^*(\mathbf{z}) \\ &= \min_{\boldsymbol{\gamma},\mathbf{z}\succeq\mathbf{0}} \sum_i \Big(\frac{\mathbf{x}_i^T\mathbf{B}_i^{-1}\mathbf{x}_i}{\gamma_i} + z_i\gamma_i\Big) - h^*(\mathbf{z}). \end{aligned} \tag{17}$$

Minimizing (17) over γ_i, we have

$$\gamma_i = z_i^{-\frac{1}{2}}\sqrt{\mathbf{x}_i^T\mathbf{B}_i^{-1}\mathbf{x}_i} \quad (\forall i) \tag{18}$$

Substituting (18) into (17) leads to

$$g_{\mathrm{c}}(\mathbf{x}) = \min_{\mathbf{z}\succeq\mathbf{0}} \sum_i \big(2z_i^{\frac{1}{2}}\sqrt{\mathbf{x}_i^T\mathbf{B}_i^{-1}\mathbf{x}_i}\big) - h^*(\mathbf{z}). \tag{19}$$

Using (19), the problem (14) now becomes:

$$\begin{aligned} \mathbf{x} &= \arg\min_{\mathbf{x}} \|\mathbf{y}-\boldsymbol{\Phi}\mathbf{x}\|_2^2 \\ &\quad +\lambda\Big[\min_{\mathbf{z}\succeq\mathbf{0}} \sum_i \big(2z_i^{\frac{1}{2}}\sqrt{\mathbf{x}_i^T\mathbf{B}_i^{-1}\mathbf{x}_i}\big) - h^*(\mathbf{z})\Big]. \end{aligned} \tag{20}$$

To further simplify the expression, we now calculate the optimal value of $z_i^{\frac{1}{2}}$. However, we need not calculate this value from the above expression. According to the duality property, from the relation (16) we can directly obtain the optimal value as follows:

$$\begin{aligned} z_i^{\frac{1}{2}} &= \Big(\frac{\partial \log|\lambda \mathbf{I} + \mathbf{\Phi}\mathbf{\Sigma}_0\mathbf{\Phi}^T|}{\partial \gamma_i}\Big)^{\frac{1}{2}} \\ &= \Big(\mathrm{Tr}\big[\mathbf{B}_i \mathbf{\Phi}^{iT}\big(\lambda\mathbf{I} + \mathbf{\Phi}\mathbf{\Sigma}_0\mathbf{\Phi}^T\big)^{-1}\mathbf{\Phi}^i\big]\Big)^{\frac{1}{2}}. \end{aligned} \tag{21}$$

Note that z_i is a function of $\boldsymbol{\gamma}$, while according to (18) γ_i is a function of $\mathbf{x}_i$ (and z_i). This means that the problem (20) should be solved in an iterative way. In the k-th iteration, having used the update rules (18) and (21) to obtain $(z_i^{(k)})^{1/2}$, we need to solve the following optimization problem:

$$\mathbf{x}^{(k+1)} = \arg\min_{\mathbf{x}} \|\mathbf{y} - \mathbf{\Phi}\mathbf{x}\|_2^2 + \lambda \sum_i w_i^{(k)} \sqrt{\mathbf{x}_i^T \mathbf{B}_i^{-1}\mathbf{x}_i}, \tag{22}$$

where $w_i^{(k)} \triangleq 2(z_i^{(k)})^{1/2}$. And the resulting $\mathbf{x}^{(k+1)}$ will be used to update γ_i and z_i, which are in turn used to calculate the solution in the next iteration.

The solution to (22) can be calculated using any Group-Lasso type algorithm. To see this, let $\mathbf{u}_i \triangleq w_i^{(k)}\mathbf{B}_i^{-1/2}\mathbf{x}_i$, $\mathbf{u} \triangleq [\mathbf{u}_1^T, \cdots, \mathbf{u}_g^T]^T$ and $\mathbf{H} \triangleq \mathbf{\Phi} \cdot \mathrm{diag}\{\mathbf{B}_1^{1/2}/w_1^{(k)}, \cdots, \mathbf{B}_g^{1/2}/w_g^{(k)}\}$. Then the problem (22) can be transformed to the following one:

$$\mathbf{u}^{(k+1)} = \arg\min_{\mathbf{u}} \|\mathbf{y} - \mathbf{H}\mathbf{u}\|_2^2 + \lambda \sum_i \|\mathbf{u}_i\|_2. \tag{23}$$

Now each iteration is a standard Group-Lasso type problem, while the whole algorithm is an iterative reweighted algorithm.

In the above development we did not consider the learning rules for the regularizers λ and $\mathbf{B}_i$. In fact, their estimation greatly benefits from this iterative reweighted form. Since each iteration is a Group-Lasso type problem, the optimal value of λ can be automatically selected in the Group Lasso framework [18]. Also, since each iteration provides a block sparse solution, which is close to the true solution, $\mathbf{B}_i$ can be directly estimated from the solution of the previous iteration. In particular, each nonzero block in the previous solution can be treated as an AR(1) process, and its AR coefficient is thus estimated. The AR coefficients associated with all the nonzero blocks are averaged [2], and the average value, denoted by $\bar{r}$, is used to construct each $\widehat{\mathbf{B}}_i$ according to (9).

The above algorithm is denoted by **BSBL-ℓ_1**. It can be seen as a hybrid of a BSBL algorithm and a Group-Lasso type algorithm. On the one hand, it has the ability to adaptively learn and exploit intra-block correlation for better performance, as BSBL-EM and BSBL-BO. On the other hand, since it only

[2] The averaging is important. Otherwise, the algorithm may have poor performance.

takes few iterations (generally about 2 to 5 iterations in noisy environments) and each iteration can be implemented by any efficient Group-Lasso type algorithm, it is much faster and is more suitable for large-scale datasets than BSBL-EM and BSBL-BO.

The algorithm also provides insights if we want to equip Group-Lasso type algorithms with the ability to exploit intra-block correlation for better recovery performance. We can consider this iterative reweighted method and change the ℓ_2 norm of $\mathbf{x}_i$, i.e., $\|\mathbf{x}_i\|_2$, to the Mahalanobis distance type measure $\sqrt{\mathbf{x}_i^T \mathbf{B}_i^{-1} \mathbf{x}_i}$.

IV. Algorithms When the Block Partition is Unknown

Now we extend the BSBL framework to address the situation when the block partition is unknown. For the algorithm development, *we assume that all the blocks are of equal size h and the nonzeros blocks are arbitrarily located*. Later we will see that the approximation of equal block size is not limiting. Note that though the resulting algorithms are not very sensitive to the choice of h, algorithmic performance can be further improved if a suitable value of h is selected. We will comment more on h later.

Given the identical block size h, there are $p \triangleq N - h + 1$ possible (overlapping) blocks in $\mathbf{x}$. The i-th block starts at the i-th element of $\mathbf{x}$ and ends at the $(i + h - 1)$-th element. All the nonzero elements of $\mathbf{x}$ lie within a subset of these blocks. Similar to Section III, for the i-th block, we assume it satisfies a multivariate Gaussian distribution with the mean given by $\mathbf{0}$ and the covariance matrix given by $\gamma_i \mathbf{B}_i$, where $\mathbf{B}_i \in \mathbb{R}^{h \times h}$. So the prior of $\mathbf{x}$ has the form: $p(\mathbf{x}) \sim \mathcal{N}_x(\mathbf{0}, \mathbf{\Sigma}_0)$. Note that due to the overlapping locations of these blocks, $\mathbf{\Sigma}_0$ is no longer a block diagonal matrix. It has the structure that each $\gamma_i \mathbf{B}_i$ lies along the principal diagonal of $\mathbf{\Sigma}_0$ and overlaps other neighboring $\gamma_j \mathbf{B}_j (j \neq i)$. Thus, we cannot directly use the BSBL framework and need to make some modifications.

To facilitate the use of the BSBL framework, we expand the covariance matrix $\mathbf{\Sigma}_0$ as follows:

$$\widetilde{\mathbf{\Sigma}}_0 = \mathrm{diag}\{\gamma_1 \mathbf{B}_1, \cdots, \gamma_p \mathbf{B}_p\} \in \mathbb{R}^{ph \times ph} \tag{24}$$

Note that $\gamma_i \mathbf{B}_i$ no longer overlaps other $\gamma_j \mathbf{B}_j (i \neq j)$. The definition of $\widetilde{\mathbf{\Sigma}}_0$ implies the following decomposition of $\mathbf{x}$:

$$\mathbf{x} = \sum_{i=1}^{p} \mathbf{E}_i \mathbf{z}_i, \tag{25}$$

where $\mathbf{z}_i \in R^{h \times 1}$, $E\{\mathbf{z}_i\} = \mathbf{0}$, $E\{\mathbf{z}_i \mathbf{z}_j^T\} = \delta_{i,j} \gamma_i \mathbf{B}_i$ ($\delta_{i,j} = 1$ if $i = j$; otherwise, $\delta_{i,j} = 0$), and $\mathbf{z} \triangleq [\mathbf{z}_1^T, \cdots, \mathbf{z}_p^T]^T \sim \mathcal{N}_z(\mathbf{0}, \widetilde{\mathbf{\Sigma}}_0)$. $\mathbf{E}_i \in \mathbb{R}^{N \times h}$ is a zero matrix except that the part from its i-th row to $(i + h - 1)$-th row is replaced by the identity matrix $\mathbf{I}$. Then the original model (1) can be expressed as:

$$\mathbf{y} = \sum_{i=1}^{p} \mathbf{\Phi} \mathbf{E}_i \mathbf{z}_i + \mathbf{v} \triangleq \mathbf{A} \mathbf{z} + \mathbf{v}, \tag{26}$$

where $\mathbf{A} \triangleq [\mathbf{A}_1, \cdots, \mathbf{A}_p]$ with $\mathbf{A}_i \triangleq \mathbf{\Phi}\mathbf{E}_i$. Now the new model (26) is a block sparse model and can be solved by the BSBL framework. Thus, following the development of BSBL-EM, BSBL-BO, and BSBL-ℓ_1, we obtain algorithms for this expanded model, which are called **EBSBL-EM**, **EBSBL-BO**, and **EBSBL-ℓ_1**, respectively.

In the derivation above we assume that all blocks have the equal known size, h. However, this assumption is not crucial for practical use. When the size of a nonzero block of $\mathbf{x}$, say $\mathbf{x}_j$, is greater than or equal to h, it can be recovered by a set of (overlapped) $\mathbf{z}_i$ ($i \in \mathcal{S}$, $\mathcal{S}$ is a non-empty set). When the size of $\mathbf{x}_j$ is less than h, it can be recovered by a $\mathbf{z}_i$ for some i. In this case, since the size of $\mathbf{z}_i$ is greater than the size of $\mathbf{x}_j$, the elements in $\mathbf{z}_i$ which do not overlap with elements of $\mathbf{x}_j$ are very close to zero. The experiments in Section V and in [13] show that different values of h lead to similar performance.

The above insight also implies that even if the block partition is unknown, one can partition a signal into a number of non-overlapping blocks with user-defined block sizes, and then perform the BSBL algorithms. Nonetheless, performance of the BSBL algorithms are generally more sensitive to the block sizes than the EBSBL algorithms when recovering block sparse signals [19] [3].

Use of the expanded model when the block partition is unknown is quite different from existing approaches [7]–[9]. Our new approach has several advantages. Firstly, it simplifies the algorithms, which, in turn, increases robustness in noisy environments, as shown in Section V. Secondly, it facilitates exploitation of intra-block correlation. Intra-block correlation is common in practical applications. Exploiting such correlation can significantly improve performance, yielding an advantage to our approach over existing methods which ignore intra-block correlation.

V. Experiments

Due to space limitations, we only present some representative experimental results based on computer simulations [4]. Experiments on real-world data can be found in [10].

In the following, each experiment was repeated for 400 trials. In each trial the matrix $\mathbf{\Phi}$ was generated as a zero mean random Gaussian matrix with columns normalized to unit ℓ_2 norm. In noisy experiments the Normalized Mean Square Error (NMSE) was used as a performance index, defined by $\|\widehat{\mathbf{x}} - \mathbf{x}_{\text{gen}}\|_2^2 / \|\mathbf{x}_{\text{gen}}\|_2^2$, where $\widehat{\mathbf{x}}$ was the estimate of the true signal $\mathbf{x}_{\text{gen}}$. In noiseless experiments the

[3] When directly recovering non-sparse signals, performance of the BSBL algorithms are not sensitive to block sizes [10].

[4] Matlab codes can be downloaded at `http://dsp.ucsd.edu/~zhilin/BSBL.html`.

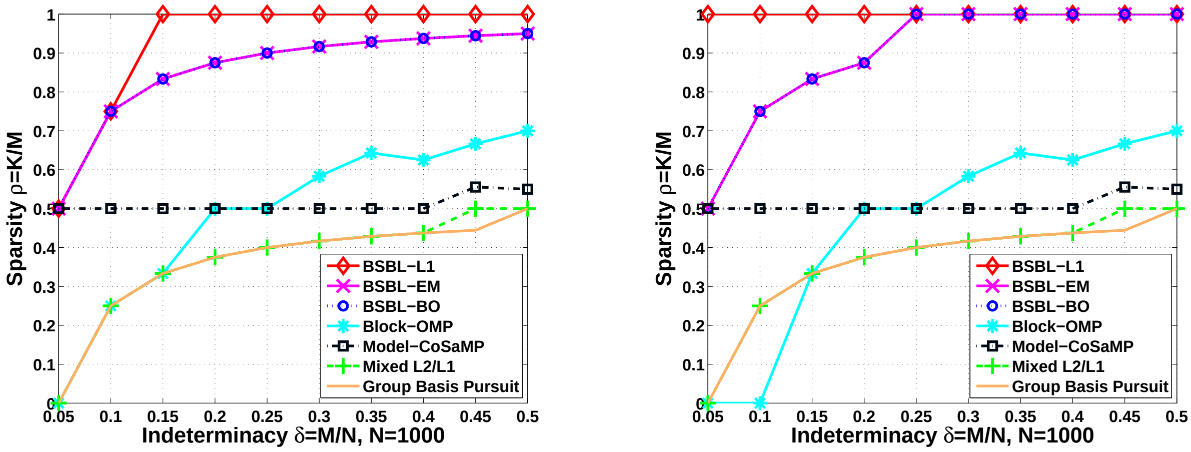

(a) Intra-Block Correlation: 0

(b) Intra-Block Correlation: 0.95

Fig. 1. Empirical 99% phase transitions of all the algorithms (a) when the intra-block correlation was 0, and (b) when the intra-block correlation was 0.95. Each point on a phase transition curve corresponds to the success rate larger than or equal to 0.99.

success rate was used as a performance index, defined as the percentage of successful trials in the 400 trials (A successful trial was defined as the one when $\mathrm{NMSE} \leq 10^{-5}$).

In noiseless experiments, we chose the Mixed ℓ_2/ℓ_1 Program [6] to solve (23) in each iteration of BSBL-ℓ_1; in noisy experiments, we chose the Group Basis Pursuit for this purpose. For all of our algorithms, when calculating r, instead of using the original formula $r = \frac{m_1}{m_0}$, the formula $r \triangleq \mathrm{sign}(\frac{m_1}{m_0}) \min\{|\frac{m_1}{m_0}|, 0.99\}$ was used to ensure that the calculated r satisfies $-1 < r < 1$. The same modification applies to $\bar{r}$.

A. Phase Transition

We first examined empirical phase transitions [20] [5] in exact recovery of block sparse signals in noiseless environments for our three BSBL algorithms, Block-OMP, Model-CoSaMP, the Mixed ℓ_2/ℓ_1 Program, and Group Basis Pursuit. The phase transition is generally used to illustrate how sparsity level (defined as $\rho = K/M$, where K is the number of nonzero elements in $\mathbf{x}$) and indeterminacy (defined as $\delta = M/N$) affect each algorithm's success in exact recovery of sparse signals. Each point on the plotted

[5] The phase transition graph was initially used to describe each algorithm's ability to recover a sparse signal with no structure. In this experiment it was used to describe each algorithm's ability to recover a sparse signal with a block structure.

phase transition curve corresponds to an algorithm's success rate greater than or equal to 99% in 400 trials. Above the curve the success rate sharply drops.

In the experiment we varied the indeterminacy $\delta = M/N$ from 0.05 to 0.5 with N fixed to 1000. For each M and N, a block sparse signal was generated, which consisted of 40 blocks with an identical block size of 25 elements. The number of nonzero blocks varied from 1 to 20; thus the number of nonzero elements varied from 25 to 500. The locations of the nonzero blocks were determined randomly. The block partition was known to the algorithms, but the number of nonzero blocks and their locations were unknown to the algorithms. Each nonzero block was generated by a multivariate Gaussian distribution with zero mean and covariance matrix $\mathbf{\Sigma}_{\mathrm{gen}}$. By manipulating the covariance matrix, and thus changing intra-block correlation, we examined the effect of intra-block correlation on each algorithm's phase transition.

We first considered the situation when the intra-block correlation was 0 (i.e., $\mathbf{\Sigma}_{\mathrm{gen}} = \mathbf{I}$). The empirical phase transition curves of all the algorithms are shown in Fig.1 (a). We can see that the three BSBL algorithms had the best performance, and the phase transition curves of BSBL-EM and BSBL-BO were identical. It is worth noting that when $\delta \geq 0.15$, BSBL-ℓ_1 exactly recovered block sparse signals with $\rho = 1$ with a high success rate ($\geq 99\%$).

The results become more interesting when the intra-block correlation was 0.95 (that is, $\mathbf{\Sigma}_{\mathrm{gen}} = \mathrm{Toeplitz}([1, 0.95, \cdots, 0.95^{24}])$). The empirical phase transition curves are shown in Fig.1 (b), where all the three BSBL algorithms had improved performance. BSBL-ℓ_1 exactly recovered sparse signals with $\rho = 1$ even for $\delta < 0.15$. BSBL-EM and BSBL-BO could exactly recover sparse signals with $\rho = 1$ when $\delta \geq 0.25$. In contrast, all the four non-BSBL algorithms showed little change in performance when the intra-block correlation changed from 0 to 0.95.

These results are very interesting and surprising, since this may be the first time that an algorithm shows the ability to recover a block sparse signal of M nonzero elements from M measurements with a high success rate ($\geq 99\%$). Obviously, exploiting block structure and intra-block correlation plays a crucial role here, indicating the advantages of the BSBL framework.

B. *Benefit of Exploiting Intra-Block Correlation*

The above results suggest there is a benefit to exploiting intra-block correlation. To further clarify this, another noiseless experiment was carried out. The matrix $\mathbf{\Phi}$ was of the size 100×300. The signal consisted of 75 blocks with an identical size of 4 elements. Only 20 of the blocks were nonzero. All the nonzero blocks had the same intra-block correlation (generated as in Section V-A) ranging from -0.99 to 0.99. Different from the first experiment, each nonzero block was further normalized to unit ℓ_2 norm in

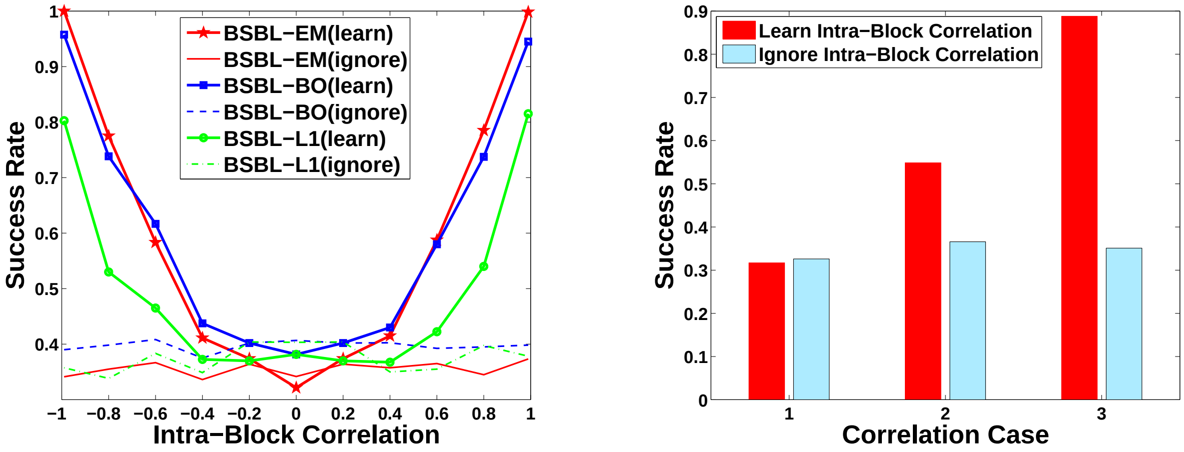

(a)

(b)

Fig. 2. (a) shows the benefit of exploiting the intra-block correlation. (b) shows the performance of BSBL-EM for three correlation conditions.

order to remove the interference caused by different ℓ_2 norms of the blocks.

BSBL-EM, BSBL-BO and BSBL-ℓ_1 were applied with and without correlation exploitation. In the first case, they adaptively learned and exploited the intra-block correlation. In the second case, they ignored the correlation, i.e., fixing $\mathbf{B}_i = \mathbf{I}(\forall i)$.

The results are shown in Fig.2 (a). First, we see that exploiting the intra-block correlation greatly improved the performance of the BSBL algorithms. Second, when ignoring the intra-block correlation, the performance of the BSBL algorithms showed no obvious relation to the correlation [6]. In other words, no obvious negative effect is observed if ignoring the intra-block correlation. Note that the second observation is quite different from the observation on *temporal correlation* in MMV models [11], where we found that if temporal correlation is not exploited, algorithms have poorer performance with increasing

[6] This phenomenon can also be observed from the performance of the compared algorithms in Section V-A, where their performance had little change when intra-block correlation dramatically varied.

temporal correlation values [7].

In the previous experiment all the nonzero blocks had the same intra-block correlation. We might then ask whether the proposed algorithms can still succeed when the intra-block correlation for nonzero blocks is not homogenous. To answer this question, we considered three possible cases for choosing intra-block correlation for each nonzero block: (1) correlation values were chosen uniformly from -1 to 1; (2) correlation values were chosen uniformly from 0 to 1; (3) correlation values were chosen uniformly from 0.7 to 1.

BSBL-EM was then applied with and without correlation exploitation, as described in the previous experiment. The results are shown in Fig.2 (b), with the three correlation cases indicated by ‘Case 1’, ‘Case 2’, and ‘Case 3’, respectively. We can see in Case 3 (least variation in intra-block correlation) the benefit of exploiting the correlation was significant, while in Case 1 (most variation in intra-block correlation) the benefit disappeared (but exploiting the correlation was not harmful). However, Case 1 rarely happens in practice. In most practical problems the intra-block correlation values of all nonzero blocks tends to be positive and high, which corresponds to Case 2 and Case 3.

C. Performance in Noisy Environments

We compared the BSBL algorithms, Mixed ℓ_2/ℓ_1 Program, Group Lasso, and Group Basis Pursuit at different noise levels. In this experiment $M = 128$ and $N = 512$. The generated block sparse signal was partitioned into 64 blocks with an identical block size of 8 elements. Seven blocks were nonzero, generated as in Section V-A. The intra-block correlation value for each block was uniformly randomly varied from 0.8 to 1. Gaussian white noise was added so that the SNR, defined by $\mathrm{SNR(dB)} \triangleq 20\log_{10}(\|\mathbf{\Phi}\mathbf{x}_{\mathrm{gen}}\|_2/\|\mathbf{v}\|_2)$, ranged from 5 dB to 25 dB for each generated signal. As a benchmark result, the ‘oracle’ result was calculated, which was the least-square estimate of $\mathbf{x}_{\mathrm{gen}}$ given its true support.

The results are shown in Fig.3 (a). All three BSBL algorithms exhibited significant performance gains over non-BSBL algorithms. In particular, the performance curves of BSBL-EM and BSBL-BO were nearly identical to that of the ’oracle’. The phenomenon that BSBL-ℓ_1 had slightly poorer performance

[7] The temporal correlation in an MMV model can be viewed as the intra-block correlation in the vectorized MMV model (which is a block sparse model). However, it should be noted that the sensing matrix in the vectorized MMV model has the specific structure $\mathbf{\Phi} \otimes \mathbf{I}_L$ [11], where $\mathbf{\Phi}$ is the sensing matrix in the original MMV model, $\otimes$ indicates the Kronecker product, $\mathbf{I}_L$ is the identity matrix with the dimension $L \times L$, and L is the number of measurement vectors in the MMV model. This structure is not present in the block sparsity model considered in this work and is believed to account for the different behavior with respect to the correlation.

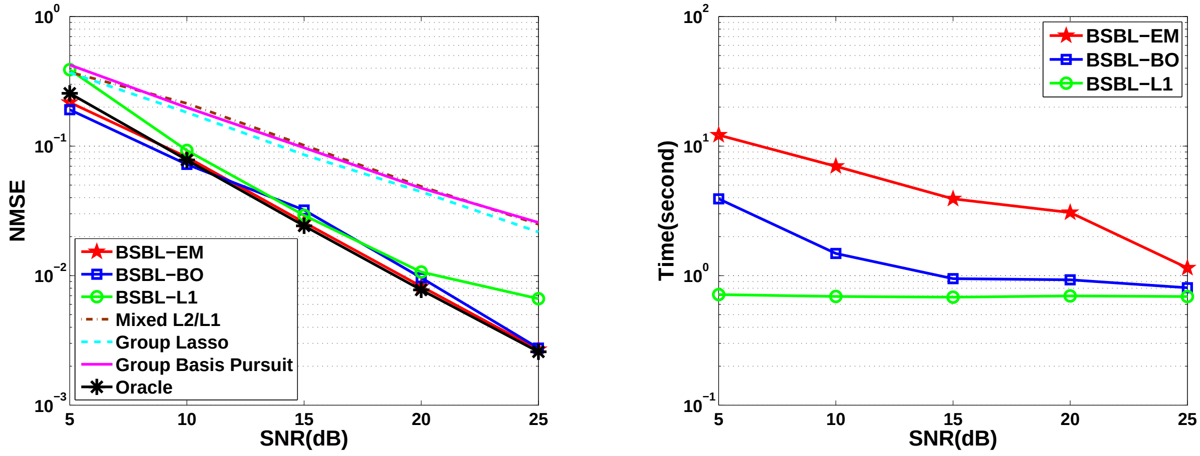

(a)

(b)

Fig. 3. (a) Performance comparison in different noise levels. (b) Comparison of the computational speed of the three BSBL algorithms in the noisy experiment.

at low SNR and high SNR situations is due to some sub-optimal default parameters in the Group Basis Pursuit program [5]. We found the phenomenon disappeared when using other software. Figure 3 (b) gives the speed comparison of the three algorithms on a computer with dual-core 2.8 GHz CPU, 6.0 GiB RAM, and Windows 7 OS. It shows BSBL-ℓ_1 was the fastest due to the use of Group Basis Pursuit in its inner loop.

D. Performance When Block Partition Is Unknown

We set up a noisy experiment to compared all of our algorithms with StructOMP (given the number of nonzero elements), BM-MAP-OMP (given the true noise variance), and CluSS-MCMC, under conditions where the block partitioning is unknown. The matrix $\mathbf{\Phi}$ was of the size 192×512. The signal $\mathbf{x}_{\mathrm{gen}}$ contained g_0 nonzero blocks with random size and random locations (not overlapping). g_0 was varied from 2 to 10. The total number of nonzero elements in $\mathbf{x}_{\mathrm{gen}}$ was fixed to 48. The intra-block correlation value for each block uniformly randomly varied from 0.8 to 1. SNR was 15 dB. As we stated in Section IV, knowledge of the block size h is not crucial in practical use. To empirically evaluate this, we calculated performance curves for all our algorithms using fixed values of $h = 4$ and $h = 8$. The results are shown in Fig.4. To improve figure readability, we only display BSBL-EM and EBSBL-BO. We also applied T-MSBL [11] here. Note that when T-MSBL is used for the block sparse signal recovery problem (1), it can be viewed as a special case of BSBL-EM with $h = 1$. The results show that our algorithms outperformed

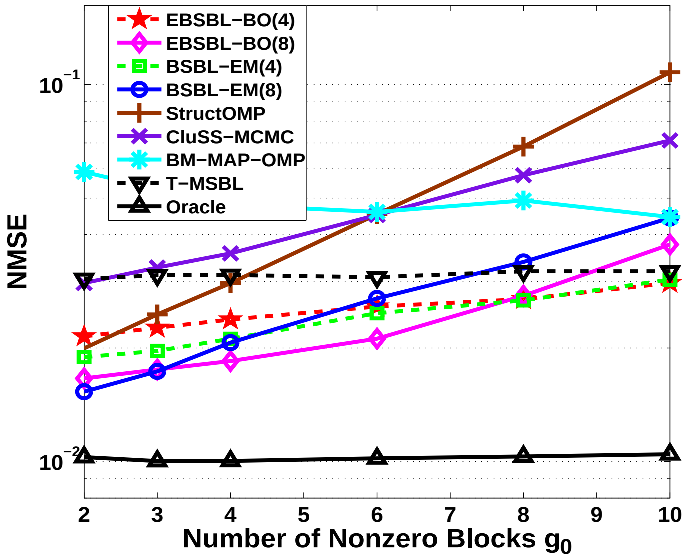

Fig. 4. Performance comparison when block partition was unknown.

StructOMP, CluSS-MCMC, and BM-MAP-OMP, and that for both BSBL-EM and EBSBL-BO, setting $h = 4$ or $h = 8$ led to similar performance.

VI. Conclusion

Using the block sparse Bayesian learning framework and its extension, we proposed a number of algorithms to recover block sparse signals when the block structure is known or unknown. These algorithms have the ability to explore and exploit intra-block correlation in signals and thereby improve performance. We experimentally demonstrated that these algorithms significantly outperform existing algorithms. The derived algorithms also suggest that the iterative reweighted framework is a promising method for Group-Lasso type algorithms to exploit intra-block correlation.

References

[1] M. Elad, *Sparse and redundant representations*. Springer Verlag, 2010.

[2] M. Yuan and Y. Lin, “Model selection and estimation in regression with grouped variables,” *J. R. Statist. Soc. B*, vol. 68, pp. 49–67, 2006.

[3] R. G. Baraniuk, V. Cevher, M. F. Duarte, and C. Hegde, “Model-based compressive sensing,” *IEEE Trans. on Information Theory*, vol. 56, no. 4, pp. 1982–2001, 2010.

[4] Y. C. Eldar, P. Kuppinger, and H. Bolcskei, “Block-sparse signals: uncertainty relations and efficient recovery,” *IEEE Trans. on Signal Processing*, vol. 58, no. 6, pp. 3042–3054, 2010.

[5] E. Van Den Berg and M. Friedlander, "Probing the pareto frontier for basis pursuit solutions," *SIAM Journal on Scientific Computing*, vol. 31, no. 2, pp. 890–912, 2008.

[6] Y. C. Eldar and M. Mishali, "Robust recovery of signals from a structured union of subspaces," *IEEE Trans. on Information Theory*, vol. 55, no. 11, pp. 5302–5316, 2009.

[7] J. Huang, T. Zhang, and D. Metaxas, "Learning with structured sparsity," in *ICML 2009*, 2009, pp. 417–424.

[8] L. Yu, H. Sun, J. P. Barbot, and G. Zheng, "Bayesian compressive sensing for cluster structured sparse signals," *Signal Processing*, vol. 92, no. 1, pp. 259–269, 2012.

[9] T. Peleg, Y. Eldar, and M. Elad, "Exploiting statistical dependencies in sparse representations for signal recovery," *IEEE Trans. on Signal Processing*, vol. 60, no. 5, pp. 2286–2303, 2012.

[10] Z. Zhang, T.-P. Jung, S. Makeig, and B. D. Rao, "Compressed sensing for energy-efficient wireless telemonitoring of non-invasive fetal ECG via block sparse Bayesian learning," *to appear in IEEE Trans. on Biomedical Engineering*.

[11] Z. Zhang and B. D. Rao, "Sparse signal recovery with temporally correlated source vectors using sparse Bayesian learning," *IEEE Journal of Selected Topics in Signal Processing*, vol. 5, no. 5, pp. 912–926, 2011.

[12] S. F. Cotter, B. D. Rao, K. Engan, and K. Kreutz-Delgado, "Sparse solutions to linear inverse problems with multiple measurement vectors," *IEEE Trans. on Signal Processing*, vol. 53, no. 7, pp. 2477–2488, 2005.

[13] Z. Zhang and B. D. Rao, "Recovery of block sparse signals using the framework of block sparse Bayesian learning," in *ICASSP 2012*, Japan, 2012, pp. 3345–3348.

[14] M. E. Tipping, "Sparse Bayesian learning and the relevance vector machine," *J. of Mach. Learn. Res.*, vol. 1, pp. 211–244, 2001.

[15] P. Stoica and P. Babu, "SPICE and LIKES: Two hyperparameter-free methods for sparse-parameter estimation," *Signal Processing*, vol. 92, no. 7, pp. 1580–1590, 2012.

[16] Z. Zhang and B. D. Rao, "Exploiting correlation in sparse signal recovery problems: Multiple measurement vectors, block sparsity, and time-varying sparsity," in *ICML 2011 Workshop on Structured Sparsity: Learning and Inference*, 2011. [Online]. Available: arXiv:1105.0725

[17] D. Wipf and S. Nagarajan, "Iterative reweighted ℓ_1 and ℓ_2 methods for finding sparse solutions," *IEEE Journal of Selected Topics in Signal Processing*, vol. 4, no. 2, pp. 317–329, 2010.

[18] R. Tibshirani, J. Bien, J. Friedman, and et al, "Strong rules for discarding predictors in lasso-type problems," *J. R. Statist. Soc. B*, vol. 74, 2012.

[19] Z. Zhang, "Sparse signal recovery exploiting spatiotemporal correlation," *Ph.D. Theis, University of California, San Diego*, 2012.

[20] D. Donoho and J. Tanner, "Observed universality of phase transitions in high-dimensional geometry, with implications for modern data analysis and signal processing," *Philosophical Transactions of the Royal Society A*, vol. 367, no. 1906, pp. 4273–4293, 2009.